Characterization of sEMG Spectral Properties During Lower Limb Muscle Activation

Costa-Garcia Alvaro[1][a] and Shimoda Shingo[2][b]

[1]National Institute of Advanced Industrial Science and Technology (AIST) Kashiwa II Campus, University of Tokyo,
6-2-3 Kashiwanoha, Kashiwa, Chiba 277-0882, Japan
[2]Nagoya University Graduate School of Medicine 64 Tsutumai, Showa-ku, Nagoya 466-8550, Japan

Keywords: Electromyography, Muscle Contraction Types, Artifacts.

Abstract: The analysis of biological data is an effective way to extract implicit information about the human physiological condition, representing the performance of daily tasks. The use of this information as feedback for robotic systems can contribute to a smoother transition into societies with a higher level of human-robot collaboration. Superficial electromyography (sEMG) could be a powerful ally in this field, as muscle activity serves as a window into our neural system and can be measured non-invasively with relative ease. In this work, our objective is to extract spectral features that enable the classification between isometric and isotonic muscle contractions. The switching between these types of contractions during human motion has been widely linked to various physical conditions, such as muscle pain, fall prediction, postural imbalances, and stress. To achieve this goal, we recorded muscle activity during both isometric and isotonic contractions under various conditions. We conducted a time-frequency analysis on the data collected from five lower limb muscles of four healthy subjects to extract significantly relevant features containing the necessary information to discriminate between these two types of muscle activations. Our results suggest that this discrimination can be achieved through the analysis of two spectral features: the median frequency and the power contained in the frequency range between 11 and 32 Hz. Furthermore, the inclusion of the peak frequency as a third feature also enables the detection of low-frequency motion artifacts.

1 INTRODUCTION

The development of increasingly efficient and intuitive systems has enabled the progressive adoption of new technologies by large population groups. This phenomenon has opened the doors to an era in which the integration between human and technological systems will occur at a fast pace (Ritchie, 2017; Besley, 1993). Since the COVID-19 pandemic and the burden it placed on medical centers around the world, governments and health institutions have been promoting the so-called 'digital health era,' encouraging people to embrace new digital media technologies for health self-monitoring. In this direction, the integration of robotic solutions that facilitate the self-monitoring of health conditions for a wider population has been widely proposed by the scientific community (Ahmed, 2021; Yang, 2019). Furthermore, over the last few decades, there has

been an explosive increase in the development of robotic systems for human support and augmentation (Green, 2008; Shimoda, 2022). Given the fundamental differences between the evolution-based appearance of humans and the engineering-based development of robotic systems, one of the biggest challenges in this field is finding appropriate methods for a smooth integration between these two natures. To achieve harmonious collaboration, it is necessary to establish communication channels between human and robotic systems that allow for a certain level of mutual understanding. Current scientific efforts in this direction involve the use of biological signals as control commands, feedback, and indicators for robotic systems (Bainbridge, 2021). A notable example of this approach is the Smart Wearable Robot with Bioinspired Sensory-Motor Skill (BioMot) project (Bacek, 2017; Costa, 2016), a European project developed between 2013 and 2016.

[a] https://orcid.org/0000-0003-0097-2793

[b] https://orcid.org/0000-0002-7759-7541

This project aimed to develop a lower limb exoskeleton that uses kinetic data, muscle activity, and real-time brain signals recorded from spinal cord injury patients to adapt their rehabilitation therapies to their current physical and cognitive state.

The use of muscle activity recorded from superficial electromyography (sEMG) has shown high performance when compared to other human recorded data (Li, 2020). Among the different bio-electrical signals, sEMG data contains more information about human behavior (both motor and neural data) than electrocardiogram (ECG) or electrooculography (EoG), and its measurement can be done with increasingly affordable and easy-to-set-up systems compared to brain signal recordings like electroencephalography (EEG). sEMG signals also exhibit a higher signal-to-noise ratio when compared to the latter systems. However, the challenge of artifact coupling on sEMG recordings during motion still needs to be addressed before their effective integration into robotic systems aimed at daily human support (Lienhard, 2015). In this regard, the current paper focuses on characterizing sEMG spectral properties under different lower limb motions to establish a ground truth that can be used in future research when these signals are employed as biofeedback communication channels for robotic devices (Lünenburger, 2007).

Therefore, the spectral characterization presented in this paper has a dual objective. On the technical side, the authors aim to highlight spectral features that will enable future researchers to detect and remove sEMG data coupled with motion artifacts, preventing this contamination from affecting the human-robot interaction stage. On the functional side, the goal is to provide a set of features that allow a classification system to distinguish between fundamentally different human motions, enabling this information to be easily shared in real-time with external devices.

For this purpose, the current research measures sEMG signals during both isometric and isotonic motions under different environmental conditions where the coupling of motion artifacts is common. Data are recorded from five different leg muscles during regular walking tasks and are separated into different pairs of motor and noise conditions. A time-frequency analysis based on the Fast-Fourier Transform was used to extract the spectral distribution associated with each task. Comparing spectral distributions between paired tasks allowed for the extraction of significant differences between experimental conditions. Finally, the observed changes in spectral distribution were used to select those features that would be most helpful in

differentiating between muscle contraction types and identifying noisy data during daily motions.

In the following section, the authors introduce the materials and methods used during this research. This information includes details about the volunteers participating in the experiment and technical information about the experimental protocol, data recording, data processing, feature extraction, and analysis methodology.

2 MATERIALS AND METHODS

2.1 Participants

Four participants, consisting of 2 men and 2 women, participated in the experiment. Their ages ranged from 27 to 46 years old, with an average age of 36.25 ± 8.42. All participants were right-footed and had no history of motor diseases. They were fully informed about the experimental conditions and provided their informed consent in accordance with the Declaration of Helsinki. The study was also approved by the ethical review board of the RIKEN research institute, with the ethical approval code: Wako3 28–13.
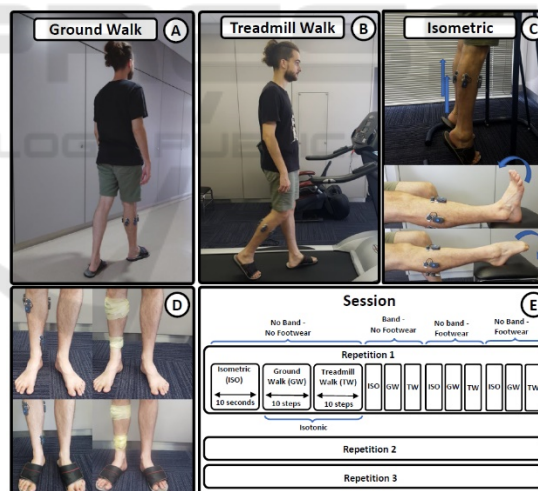

Figure 1: **Experimental Conditions and Queue.** A) Ground walking. B) Treadmill walking. C) Isometric contraction of gastrocnemius and vaslus lateralis muscle in the top image, tibialis anterior in the middle image and peroneus longus in the bottom image. D) Combination of band and no band fixation condition with the usage or not of footwear. E) Graphical representation of an experimental session composed of 3 repetitions of 12 tasks resulting form the combonantion of motion types, band fixations and foowear usage.
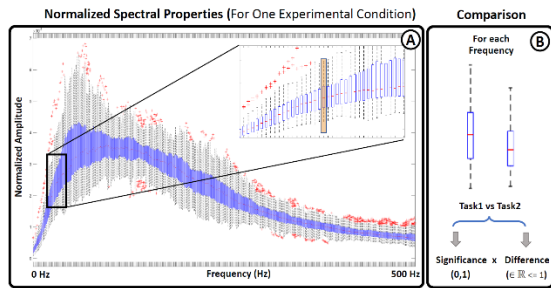
Figure 2: **Spectral Representation.** Boxplot representation of the spectral features extracted from a given experimental condition. The boxplot distribution of paired task were compared frequency by frequency using a Wilcoxon Sum-rank Test to find statistical differences between conditions.

2.2 Experimental Protocol

Each participant completed a single experimental session consisting of three repetitions of the task sequence depicted in Figure 1. Each task was defined as a combination of a motion condition (isometric contraction, ground walking, and treadmill walking - as shown in Figure 1A-C), electrode fixation system (using a band for electrode fixation or not - as depicted in Figure 1D), and footwear usage (with or without footwear - as illustrated in Figure 1E). This resulted in a total of 12 tasks per repetition, as indicated in Figure 1E. During isotonic motions (treadmill and ground walking conditions), participants were asked to walk for 10 steps, while during isometric contraction tasks, they were instructed to activate their muscles for 10 seconds. After completing the three repetitions, the sEMG data included muscle activation data from 30 steps for each task performed under isotonic motion and 30 seconds of data from tasks recorded during isometric contractions. The inclusion of different electrode fixation conditions aimed to assess motion artifacts related to the vibration of hanging electrodes caused by the momentum generated in the lower limb during gait. Additionally, the use of footwear, along with the choice between a treadmill or regular ground walking, was considered to account for spectral changes associated with the coupling of power line noise originating from the environment or other external devices.

2.3 sEMG Recordings

Muscle activity was recorded using five wireless bipolar electrodes (BTS FREEEMG; BTS Bioengineering Corp., Milan, Italy) placed on the following muscles: peroneus longus (PL), tibialis anterior (TA), vastus lateralis (VLAT),

gastrocnemius medialis (GAN), and gastrocnemius lateralis (GAL). The placement of electrodes followed the guidelines established by the Surface Electromyography for the Non-Invasive Assessment of Muscles (SENIAM) project (Stegeman, 2007). Data were digitized at a rate of 1000 Hz.

The selection of these muscles was based on criteria targeting muscles that are highly active during walking motions (Costa, 2021). These muscles were chosen because they are located in the lower part of the legs, where motion momentum is higher, and therefore, motion artifacts are also expected to be stronger.

To ensure the correct activation of the five selected muscles during all tasks, isometric contraction conditions were recorded under two different exercises, as shown in Figure 1C. The top image in Figure 1C illustrates the exercise used for the isometric activation of the GAN, GAL, and VLAT muscles, while the lower images in Figure 1C depict the position and exercise used for the TA and PL isometric contraction.

2.4 Data Processing and Feature Extraction

In this study, one of the primary objectives was to evaluate the effects of artifacts on the spectral properties of sEMG data. To ensure that the impact of motion artifacts was included in the analysis, the recorded signals did not undergo rectification or filtering.

Before performing spectral computations, each task was segmented into 10 epochs. The segmentation techniques applied to isotonic and isometric tasks differed due to their fundamental nature. For isometric contractions (where 10 seconds of data were extracted for each task), epochs were obtained as consecutive one-second segments. In the case of isotonic motion tasks, each epoch corresponded to the muscle activation produced by a single step. The starting and ending values of each segment were determined independently for each muscle using a methodology for periodic motion segmentation previously introduced in (Costa, 2020). This method identifies minima and maxima in the sEMG envelope that best align with the expected number of activations (10 steps per task in this study). It uses an iterative low-pass filtering process to adjust the cutoff frequency until the envelope synchronizes with the number of steps. The extracted points serve as markers for epoching the sEMG raw segmentation markers for epoching the sEMG raw segment data.
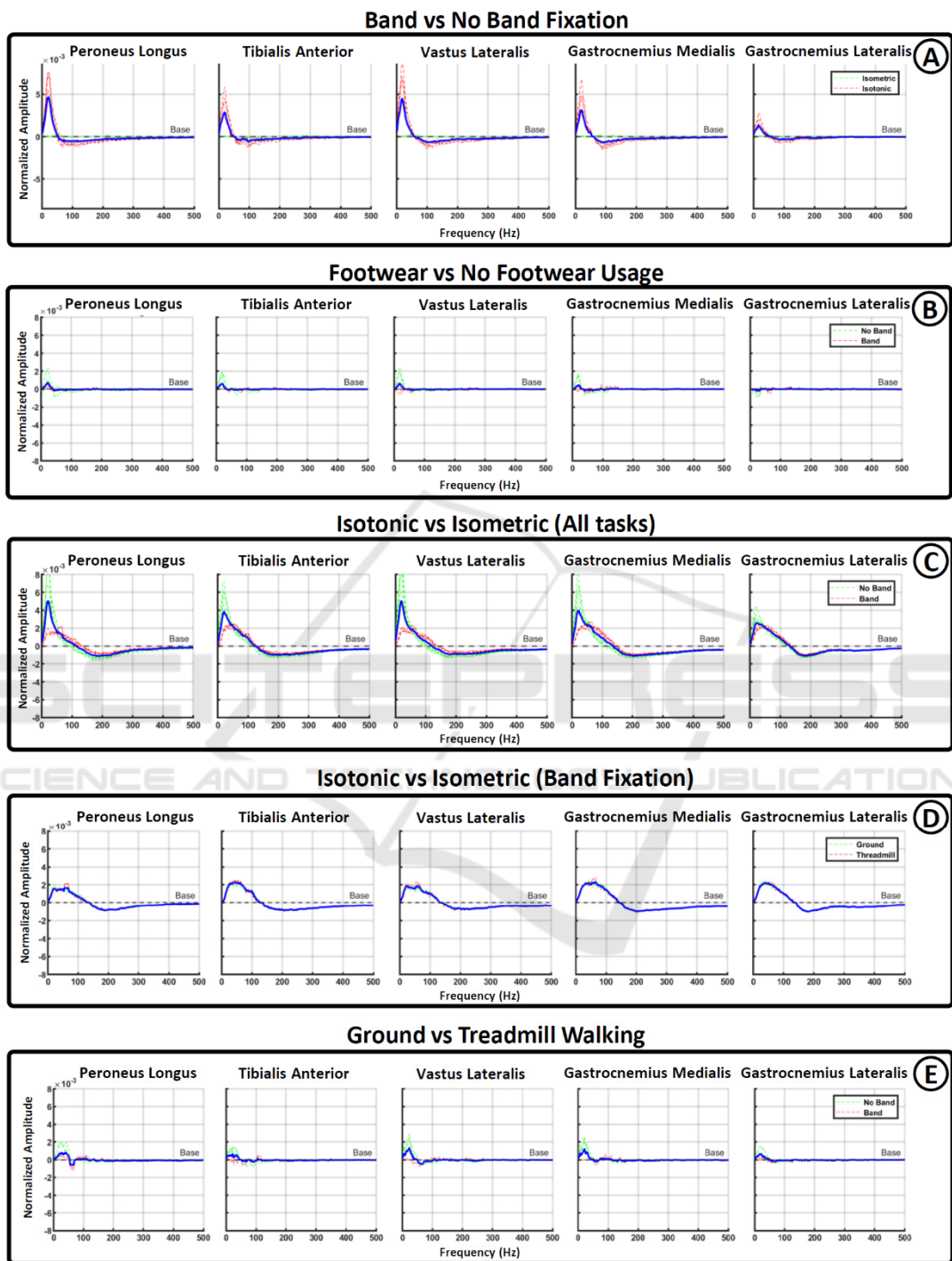
Figure 3: **Spectral differences across conditions.** Figures from A to E show the frequency range in which statistical significance was found among different pair of condition. Vertically arranged graph show the results for each one of the five muscle recorded during the experiment. Red and green lines were used to show subdivision among the conditions compared and blue lines represent average values.

Next, a Fast Fourier Transformation (FFT) was applied to each raw epoch to extract their spectral features. Additionally, the power at each frequency was divided by the total power within the range of 1-500 Hz, respecting the Nyquist criteria for not aliasing frequencies (Robinson, 1991). This normalization scales the total power of the spectrum to 1, highlighting how power is distributed within the spectrum by removing amplitude variations. This normalization allows for better comparisons between tasks and subjects in terms of spectral distribution.

Due to the observed spectral differences between the various conditions of the analyzed data (for more details, refer to the Results section), three distinct features were extracted from each normalized spectrum: a) peak frequency: this represents the single frequency value containing the highest amplitude in the spectrum; b) median frequency: This indicates the frequency value that divides the spectrum into two areas with equal power; and c) power within the range of 11 to 32 Hz: This measures the power contained within this specific frequency range.
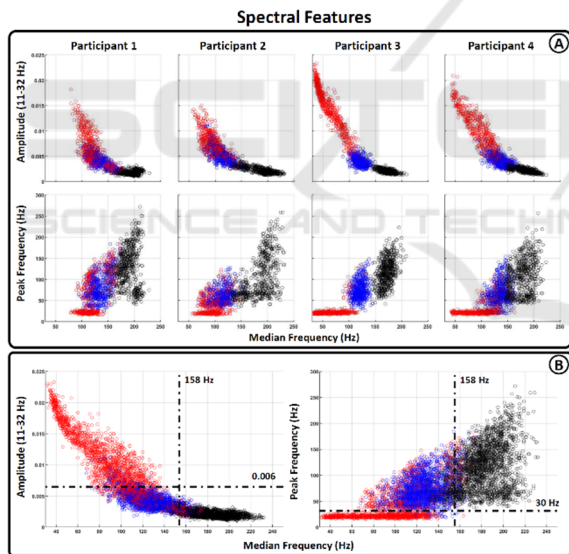

Figure 4: **Spectral features.** Bidimensional representation of the 3 spectral features extracted from the main spectral distributions. X-axis represents median frequency and Y-axis represents the normalized amplitude in the range between 11-32 Hz and the frequency recording the peak amplitude respectively. Feature were painted with three different colors to differentiate between isometric motions (black dots), isometric motion without (red dots) and with (blue) electrode fixation. A) Represent the feature extracted for each subject independently. B) Shows the average data for all participants.
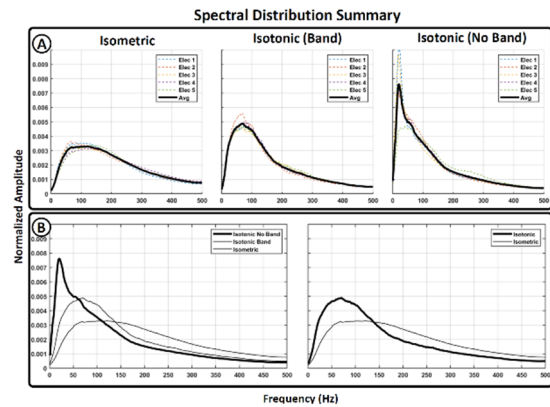

Figure 5: **Summary of main spectral distribution.** Average values associated to the main spectral distribution found after sEMG analysis. A) Isometric contraction (left graph), isotonic contraction during electrode fixation (middle graph) and isotonic contraction without electrode fixation (right graph). B) Comparison between main spectral distributions

2.5 Data Comparison

The various tasks recorded during a single session were organized into different groups to facilitate comparisons between different experimental conditions. These groupings encompassed comparisons between isometric and isotonic tasks, ground walking and treadmill walking tasks, tasks with and without a band for electrode fixation, and tasks with and without the use of footwear.

To identify statistically significant differences in the spectrum between pairs of conditions, all the spectra associated with the same condition were represented using boxplots, as illustrated in Figure 2A. The values used for the boxplot representation at each frequency were then compared between paired tasks using a Wilcoxon sum-rank test, followed by a Bonferroni-Holm correction to account for multiple comparisons (Rey, 2011; Abdi, 2010). Subsequently, the frequency values that exhibited statistical significance were represented as the difference between the median values of the respective tasks.

3 RESULTS

3.1 Spectral Shape Comparison

Figure 3 presents the results of spectral comparisons for various paired conditions. In Figure 3A, it becomes evident that the use of band fixation significantly reduces low-frequency activation, typically associated with motion artifacts. This

reduction is particularly pronounced during isotonic tasks but has minimal impact during isometric contractions. In Figure 3B, the comparison between tasks with and without footwear shows less pronounced spectral differences, primarily affecting the no-band fixation conditions. This suggests that proper electrode fixation is more critical than the type of footwear used.

Figures 3C-D compare isotonic and isometric tasks. Figure 3C includes both band and no-band fixation conditions, revealing an increased effect on lower-frequency activation associated with the no-band condition. When the no-band condition is removed (Figure 3D), it becomes apparent that isotonic motions lead to an expansion in the spectral range between 20-140 Hz compared to isometric motions. In this case, there are no notable differences between ground walking and treadmill walking.

Furthermore, Figure 3E illustrates the spectral differences between ground and treadmill walking conditions. It is noticeable that an increase in low frequencies during ground walking occurs only under the no-band fixation condition, further supporting the idea that when electrodes are securely fixed, there are no significant spectral differences between ground and treadmill walking.

Lastly, Figure 4A provides a summary of the main spectral differences observed among the analyzed conditions. The leftmost graph depicts the spectral distribution of isometric tasks for the five evaluated muscles, revealing no significant changes related to footwear or fixation conditions. The middle graph displays the spectral distribution of isotonic tasks during electrode fixation conditions, showing no significant differences between ground/treadmill walking or footwear usage. The right graph demonstrates the effects of not using a band for electrode fixation in the low frequencies of the spectrum. Electrodes 4 and 5, located in the gastrocnemius muscle with less momentum, appear less affected by lower frequency increases, further supporting the hypothesis that this activation is a consequence of motion artifacts. Figure 4B presents a comparison between the three previous spectra (left graph) and between isotonic and isometric conditions when motion artifact conditions are not included (right graph).

3.2 Feature Representation for Classification

In Figure 5B, two bidimensional graphs provide a comparison of the three extracted spectral features (peak frequency, median frequency, and normalized amplitude within the 11-32 Hz range) across different conditions. The right graph illustrates the relationship between peak and median frequencies, while the left graph compares median frequency with the power distribution in the 11-32 Hz range. Red dots represent features extracted from isotonic motions where electrodes were not fixed by the band. Blue dots show the features of isotonic motions with properly fixed electrodes. Finally, black dots represent features extracted during isometric motions.

Figure 5A presents the same features, but they are separated for each participant, which helps underscore the level of inter-subject variability in the analyzed data.

4 DISCUSSION

Our results reveal two primary changes in the spectral distribution of sEMG data under the evaluated conditions. The first change involves an increase in the power of low frequencies observed during isotonic data recordings without electrode fixation. This change is clearly depicted in Figure 3A (red dotted line) and Figure 3C (green dotted line). Importantly, this phenomenon is absent during isometric contractions (Figure 3C, red dotted line), suggesting that the rise in lower frequencies is a consequence of motion artifacts stemming from electrode vibration during walking tasks. This frequency alteration affects the range between 11 and 32 Hz, with a peak value at approximately 22 Hz, aligning with the frequency range traditionally associated with motion artifacts (Lienhard, 2015; Fratini, 2009).

The second change involves a more gradual shift between high and low frequencies when comparing isometric and isotonic contractions, particularly under electrode fixation conditions (Figure 3D). This phenomenon indicates that, for isotonic motions, there is an increase in the range between 30 and 100 Hz, compensated by a decrease between 200-300 Hz. Unlike the previous range strongly linked to motion artifacts, this affected range is much broader and has minimal overlap. Furthermore, the frequencies impacted fall within the range at which motor unit action potentials are generated (Costa, 2022). This suggests that the spectral differences between isotonic and isometric contractions arise from physiological differences rather than noise coupling.

Under band fixation conditions, no significant changes were observed between footwear conditions (Figure 3B, red dotted line) or between ground and treadmill walking (Figure 3D, red dotted line). This

indicates that the coupling of external noise sources, such as power line interference, has minimal influence on the spectral distribution of sEMG, making it easier to mitigate during recordings in daily environments.

These findings enable the classification of sEMG spectral distributions into three main groups: isometric contractions, normal isotonic contractions, and isotonic contractions with coupled motion artifacts. The spectral features of each group exhibit sufficient distinctiveness, as illustrated in Figure 5 (median frequency, peak frequency, and normalized amplitude in the 11-32 Hz range). The black, blue, and red feature clusters presented in Figure 5 suggest that differentiation should be feasible with straightforward classification techniques, enabling real-time discrimination between isometric/isotonic contractions and noisy/not noisy trials. Furthermore, our results indicate low inter-subject variability in the feature space (Figure 5A), which enhances the potential for wider generalization of the classification algorithm.

5 CONCLUSIONS

This study has identified distinct spectral features in the sEMG spectrum that enable two important outcomes: a) the discrimination between isotonic and isometric contractions, and b) the detection of low-frequency motion artifacts during walking tasks.

The differentiation between isometric and isotonic contractions has widespread applications in motor control, offering insights into various cognitive states such as pre-fall postural instability (Xi, 2017), motion-related muscle and joint pain (Neblett, 2016), stress/anxiety-related head pain and migraines (Bakal, 1977), among others. Consequently, distinguishing between these fundamental contractions represents a crucial initial step in providing robotic systems with valuable information about the cognitive state of the human. Additionally, the ability to identify signal segments contaminated by motion artifacts allows robotic devices to determine the reliability of received physiological data. As mentioned in the introduction, the challenge of motion artifact coupling is pertinent to the measurement of biosignals during human-robot interaction. Precisely detecting noisy motion trials will aid in assessing current integrative solutions and developing innovative approaches to noise reduction.

Furthermore, comparing the spectral distributions obtained in this study can facilitate future research in evaluating changes in sEMG recordings following the

integration of robotic devices into the human control loop. After further validation through a larger subject sample, future steps will involve developing a classification system that enables real-time discrimination of sEMG segments based on the extracted features and testing this system in human-robot collaborative environments.

Lastly, it's important to note that while this study primarily focuses on physiological signals, there are also many human-robot interaction solutions based on the analysis of non-bioelectrical data such as kinematic or visual information. Although these signals may not provide as much insight into the neural processes underlying human behavior, they offer benefits like easier recording and higher accuracy in determining motion start and end points. In general, the existence of such a variety of approaches is a positive aspect within the scientific community, and final integrative solutions will likely emerge from a combination of these diverse approaches.

REFERENCES

Abdi, H., "Holm's sequential Bonferroni procedure," in Encyclopedia of research design vol. 1(8), 2010, pp. 1-8.

Ahmed, S.N., "Covid, AI, and robotics—A neurologist's perspective," in Frontiers in Robotics and AI, vol 8, 2021, pp. 617426.

Bacek, T., Moltedo, M., Langlois, K., Prieto, G.A., Sanchez-Villamañan, M.C., Gonzalez-Vargas, J., Vanderborght, B., Lefeber, D. and Moreno, J.C., "BioMot exoskeleton—Towards a smart wearable robot for symbiotic human-robot interaction," in International Conference on Rehabilitation Robotics (ICORR), 2017.

Bainbridge, W.A., Nozawa, S., Ueda, R., Okada, K. and Inaba, M., "A methodological outline and utility assessment of sensor-based biosignal measurement in human-robot interaction," in International Journal of Social Robotics, vol. 4(3), 2012, pp. 303-316.

Bakal, D.A. and Kaganov, J.A., "Muscle contraction and migraine headache: psychophysiologic comparison," in Headache: The Journal of Head and Face Pain, vol. 17(5), 1977, pp. 208-215.

Besley, T., and Case A., "Modeling technology adoption in developing countries," in The American economic review, vol. 83 (2), 1993, pp. 396-402.

Costa, Á., Iáñez, E., Úbeda, A., Hortal, E., Del-Ama, A.J., Gil-Agudo, A. and Azorín, J.M., "Decoding the attentional demands of gait through EEG gamma band features," in PLoS one, vol. 11(4), 2016, pp. e0154136.

Costa-García, Á., Iáñez, E., Sonoo, M., Okajima, S., Yamasaki, H., Ueda, S. and Shimoda, S., "Segmentation and averaging of sEMG muscle activations prior to synergy extraction," in IEEE Robotics and Automation Letters vol. 5(2), 2020, pp. 3106-3112.

Costa‐García, Á., Iáñez, E., Yokoyama, M., Ueda, S., Okajima, S. and Shimoda, S., "Quantification of high and low sEMG spectral components during sustained isometric contraction," in Physiological Reports vol. 10(10), 2022, pp. e15296.

Costa-García, Á., Úbeda, A. and Shimoda, S., "Effects of Force Modulation on Large Muscles during Human Cycling." in Brain Sciences vol. 11(11), 2021, pp. 1537.

Fratini, A., Cesarelli, M., Bifulco, P. and Romano, M., "Relevance of motion artifact in electromyography recordings during vibration treatment," in Journal of Electromyography and Kinesiology, vol. 19(4), 2009, pp. 710-718.

Green, S. A., Billinghurst, M., Chen, X., and Chase, J. G, "Human-robot collaboration: A literature review and augmented reality approach in design," in International journal of advanced robotic systems, vol. 5(1), 2008, pp. 1.

Li, K., Zhang, J., Wang, L., Zhang, M., Li, J. and Bao, S., "A review of the key technologies for sEMG-based human-robot interaction systems," in Biomedical Signal Processing and Control, vol 62, 2020, pp. 102074.

Lienhard, K., Cabasson, A., Meste, O. and Colson, S.S., "sEMG during whole-body vibration contains motion artifacts and reflex activity," in Journal of sports science & medicine, vol. 14(1), 2015, pp. 54.

Lünenburger, L., Colombo, G. and Riener, R., "Biofeedback for robotic gait rehabilitation," in Journal of neuroengineering and rehabilitation, vol. 4(1), 2007, pp. 1-11.

Neblett, R., "Surface electromyographic (SEMG) biofeedback for chronic low back pain," in Healthcare, vol. 4(2), 2016, MDPI.

Rey, D. and Neuhäuser, M., "Wilcoxon-signed-rank test," in International encyclopedia of statistical science, 2011, pp. 1658-1659.

Ritchie, H., and Roser M., "Technology adoption," in Our World in Data, 2017.

Robinson, E. and Clark, D., "Sampling and the Nyquist frequency," in The Leading Edge vol. 10(3), 1991, pp. 51-53.

Shimoda, S., Jamone, L., Ognibene, D., Nagai, T., Sciutti, A., Costa-Garcia, A., Oseki, Y. and Taniguchi, T., "What is the role of the next generation of cognitive robotics?," in Advanced Robotics, vol. 36(1-2), 2022, pp. 3-16.

Stegeman, D. and Hermens, H.,"Standards for surface electromyography: The European project Surface EMG for noninvasive assessment of muscles (SENIAM)," in Enschede: Roessingh Research and Development, vol. 10, 2007, pp. 8-12.

Xi, X., Tang, M., Miran, S.M. and Luo, Z., "Evaluation of feature extraction and recognition for activity monitoring and fall detection based on wearable sEMG sensors," in Sensors, vol, 17(6), 2017, pp. 1229.

Yang, J.C., Mun, J., Kwon, S.Y., Park, S., Bao, Z. and Park, S., "Electronic skin: recent progress and future prospects for skin-attachable devices for health monitoring, robotics, and prosthetics," in Advanced Materials, vol 31(48), 2019, pp. 1904765.